

Mapping Highly Efficient Mixed-cation Pseudohalide-perovskite Solar Cells with a Scanning Transmission X-ray Microscope

Ming-Wei Lin¹, Hung-Wei Shiu¹, Kuo-Chin Wang², Ming-Hsien Li², Yu-Ling Lai¹, Takuji Ohigashi³, Nobuhiro Kosugi³, Tzung-Fang Guo², Peter Chen², and Yao-Jane Hsu^{1,2*}

¹ National Synchrotron Radiation Research Center, Hsinchu, Taiwan, R.O.C.

² Department of Photonics, National Cheng Kung University, Tainan, Taiwan, R.O.C.

³ UVSOR Synchrotron, Institute for Molecular Science, Okazaki, Japan.

* Yao-Jane Hsu, yjhsu@nsrrc.org.tw

The organic–inorganic hybrid perovskite structure has rapidly attracted much attention because of the highly efficient photovoltaic cells in which it serves as a light sensitizer [1]. The perovskites are typically metal-organic frameworks of form ABX_3 , in which A is $CH_3NH_3^+$ (MA) or $CH_3(NH_2)_2^+$ (FA) or Cs^+ , B is Pb^{2+} or Sn^{2+} , and X is I^- or Cl^- or Br^- . For example, methylammonium lead iodide ($MAPbI_3$) and its analogues exhibit novel properties such as ambipolar charge transport, a large absorption coefficient and an effective electron- or hole-diffusion length, making them suitable for photovoltaic applications. Among various perovskites, the mixed-cation lead pseudohalide perovskites were particularly successful with a large power-conversion efficiency (PCE) and satisfactory stability against moisture [2-3]. The large crystalline size with few trap states, increased entropy or decreased formation of solid solution are experimentally or theoretically proposed to interpret the origin of this high efficiency and stability. The variation of film morphologies is typically examined with a conventional TEM or SEM that provides only the bulk structure in a cross-sectional view or the surface topography in a top view. The necessity arises to improve the mapping capability to inspect the multilayer structures with a scaffold of an electron-transport layer (ETL)/perovskite/hole-transport layer (HTM) in perovskite-based solar cells. We have investigated the origin of the large PCE and the stability of mixed-cation pseudohalide perovskite solar cells using a scanning transmission x-ray microscope (STXM). In our experiments to fabricate perovskite solar cells, the mixed cation with formamidinium (FA: $HC(NH_2)_2$) and Cs cations replaced methylammonium. To improve the PCE efficiency and structural stability, we used lead thiocyanate ($Pb(SCN)_2$) as dopant so that the thiocyanate (SCN^-) anions replaced the halide ions in the tetragonal sites of the unit lattice of perovskite $FA_{0.9}Cs_{0.1}PbI_3$ solar cells. The cell devices with mesoscopic titania as scaffold/electron-transport layer and spiro-OMeTAD as hole-transport layer were examined for the photovoltaic performance under standard illumination conditions. PCE greater than 16 % was achieved with optimized $Pb(SCN)_2$ doping relative to 13.9 % for cells without $Pb(SCN)_2$. To understand the origin of this improved efficiency and structural stability, we used a STXM to examine the chemical structure and morphology. The samples of $FA_{0.9}Cs_{0.1}PbI_3$ cuboids and with varied $Pb(SCN)_2$ concentration in molar ratios 5%, and 10% were prepared in our laboratory. The NEXAFS absorption spectra and STXM images at varied absorption edges, such as the C, O, N *K*-edge and Ti *L*-edge, were recorded at BL 09A2 spectroscopy of Taiwan Light Source at NSRRC and at BL4U in UVSOR Synchrotron in Japan, respectively.

To study the effect of doping of $Pb(SCN)_2$ on the efficiency and stability, we prepared pristine perovskite $FA_{0.9}Cs_{0.1}PbI_3$ and $Pb(SCN)_2$ -doped $FA_{0.9}Cs_{0.1}PbI_3$ and spin cast them on mesoporous TiO_2 layers (mp- TiO_2) that were pre-cast on SiN membranes. Figure 1 displays STXM images of the C *K*-edge acquired at 287.6 eV, which is attributed to a C-N σ^* resonance of FA ($HC^*(NH_2)_2$) in $FA_{0.9}Cs_{0.1}PbI_3$ with $Pb(SCN)_2$ doped at 5 % (Fig. a) and 10 % (Fig. b). Compared to pristine $FA_{0.9}Cs_{0.1}PbI_3$ (that shows no contrast), the

5 %-doped $\text{FA}_{0.9}\text{Cs}_{0.1}\text{PbI}_3$ shows bright cuboids and a few black rods. In contrast, 10 % doped $\text{FA}_{0.9}\text{Cs}_{0.1}\text{PbI}_3$ expresses similar bright cuboids but more black sticks and irregular blocks that show black and grey contrast, which apparently result from too much $\text{Pb}(\text{SCN})_2$ dopant. A comparison of chemical mapping of the C *K*-edge at 287.6 eV, N *K*-edge at 400.7 eV and Ti *L*-edge at 457.9 eV for 5 % $\text{Pb}(\text{SCN})_2$ is shown in Figure 1(c), (d) and (e), respectively. Both C and N mapping, which were acquired at characteristic absorption features of $\text{FA}_{0.9}\text{Cs}_{0.1}\text{PbI}_3$ perovskite, display the same features and contrast that are not directly correlated with the distribution of mp- TiO_2 . The crystalline size of $\text{Pb}(\text{SCN})_2$ doped- $\text{FA}_{0.9}\text{Cs}_{0.1}\text{PbI}_3$ perovskite are, however, significantly decreased when grown on mp- TiO_2 . This condition indicates that $\text{Pb}(\text{SCN})_2$ and mesoporous TiO_2 play key important roles to affect the growth of perovskite crystallites. The optimized addition of $\text{Pb}(\text{SCN})_2$ is advantageous to enlarge the crystal size of $\text{FA}_{0.9}\text{Cs}_{0.1}\text{PbI}_3$ on mp- TiO_2 . To comprehend thoroughly the distribution of heterostructure layers, we display in Figure 2 the chemical maps of the N *K*-edge and Ti *L*-edge of $\text{SiN}/\text{mp-TiO}_2/5\% \text{Pb}(\text{SCN})_2$ doped- $\text{FA}_{0.9}\text{Cs}_{0.1}\text{PbI}_3$, and $\text{SiN}/\text{mp-TiO}_2/10\% \text{Pb}(\text{SCN})_2$ doped- $\text{FA}_{0.9}\text{Cs}_{0.1}\text{PbI}_3$, which are maps of optical density (OD) obtained at the characteristic absorption

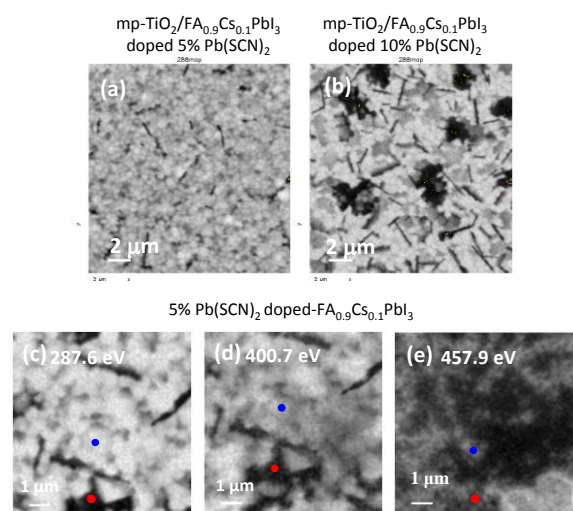


Figure 1. STXM OD images of C *K*-edge at 287.6 eV for (a) $\text{SiN}/\text{mp-TiO}_2/5\% \text{Pb}(\text{SCN})_2$ doped- $\text{FA}_{0.9}\text{Cs}_{0.1}\text{PbI}_3$, and (b) $\text{SiN}/\text{mp-TiO}_2/10\% \text{Pb}(\text{SCN})_2$ doped- $\text{FA}_{0.9}\text{Cs}_{0.1}\text{PbI}_3$. The OD images of (c) C *K*-edge at 287.6 eV, (d) N *K*-edge at 400.7 eV and (e) Ti *L*-edge at 457.9 eV for 5% $\text{Pb}(\text{SCN})_2$ doped- $\text{FA}_{0.9}\text{Cs}_{0.1}\text{PbI}_3$. All images have subtracted the pre-edge image.

features of $\text{FA}_{0.9}\text{Cs}_{0.1}\text{PbI}_3$ and mp- TiO_2 . There are notable additional sticks and large aggregated blocks, as shown in red and yellow colors in the composite images determined as TiO_2 nanoparticles that have a uniform diameter 2~5 μm and appear to be more uniformly dispersed in 5 % $\text{Pb}(\text{SCN})_2$ doped- $\text{FA}_{0.9}\text{Cs}_{0.1}\text{PbI}_3$. 5 % $\text{Pb}(\text{SCN})_2$ doped- $\text{FA}_{0.9}\text{Cs}_{0.1}\text{PbI}_3$ has hence an effective charge transfer between perovskite and TiO_2 . The STXM results indicate that the interaction between mp- TiO_2 and perovskite plays a key role in determining the PCE performance. The morphology variation of perovskite is correlated with mp- TiO_2 and $\text{Pb}(\text{SCN})_2$, which illustrates that the interaction between mp- TiO_2 and perovskite is not favored to grow large and defect-free perovskite layers for charge transfer.

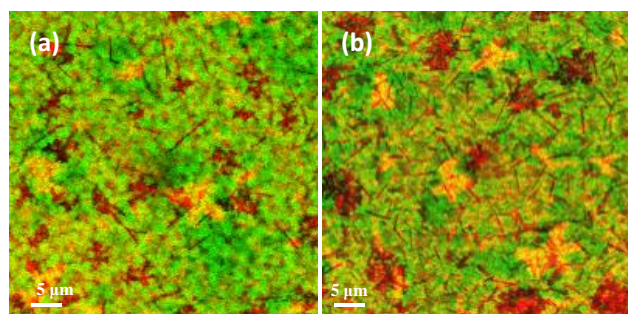


Figure 2. Chemical mapping of Ti *L*-edge (red) and N *K*-edge (green) of (a) $\text{SiN}/\text{mp-TiO}_2/5\% \text{Pb}(\text{SCN})_2$ doped- $\text{FA}_{0.9}\text{Cs}_{0.1}\text{PbI}_3$, and (b) $\text{SiN}/\text{mp-TiO}_2/10\% \text{Pb}(\text{SCN})_2$ doped- $\text{FA}_{0.9}\text{Cs}_{0.1}\text{PbI}_3$.

of $\text{FA}_{0.9}\text{Cs}_{0.1}\text{PbI}_3$ perovskite, display the same features and contrast that are not directly correlated with the distribution of mp- TiO_2 . The crystalline size of $\text{Pb}(\text{SCN})_2$ doped- $\text{FA}_{0.9}\text{Cs}_{0.1}\text{PbI}_3$ perovskite are, however, significantly decreased when grown on mp- TiO_2 . This condition indicates that $\text{Pb}(\text{SCN})_2$ and mesoporous TiO_2 play key important roles to affect the growth of perovskite crystallites. The optimized addition of $\text{Pb}(\text{SCN})_2$ is advantageous to enlarge the crystal size of $\text{FA}_{0.9}\text{Cs}_{0.1}\text{PbI}_3$ on mp- TiO_2 . To comprehend thoroughly the distribution of heterostructure layers, we display in Figure 2 the chemical maps of the N *K*-edge and Ti *L*-edge of $\text{SiN}/\text{mp-TiO}_2/5\% \text{Pb}(\text{SCN})_2$ doped- $\text{FA}_{0.9}\text{Cs}_{0.1}\text{PbI}_3$, and $\text{SiN}/\text{mp-TiO}_2/10\% \text{Pb}(\text{SCN})_2$ doped- $\text{FA}_{0.9}\text{Cs}_{0.1}\text{PbI}_3$, which are maps of optical density (OD) obtained at the characteristic absorption

References

- [1] M. A. Green, et al., *Nat. Photonics*, 8, 506 (2014).
- [2] M.-W. Lin, et al., *Adv. Mater. Interfaces*, 3, 1600135 (2016).
- [3] Z. Xiao, et al., *Adv. Mater.*, 26, 6503 (2014).
- [4] The authors acknowledge funding from the Ministry of Science and Technology, National Synchrotron Radiation Research Center and the UVSOR-RIKEN collaboration program.